Ocean & Sea Ice SAF

ERS Scatterometer Ambiguity Removal Scheme Comparison

Ad Stoffelen, KNMI
Siebren de Haan, KNMI
Yves Quilfen, IFREMER
Harald Schyberg, DNMI

Contents

Scatterometer Ambiguity Removal Scheme Comparison

ABSTRACT

Scatterometers provide ambiguous winds and ambiguity removal (AR) schemes exist to select a unique solution from the set of ambiguous wind vectors based on spatial filtering constraints. Several of such AR schemes have been developed in the past and based on subjective arguments several of these schemes are in routine use. Here we present an objective method to compare AR schemes. We consider different AR schemes for scatterometer data, compare them for different wind speed regimes, geographical region, and dynamical cases, in order to provide both an objective and subjective judgement of their relative merits. We find that AR schemes are not particularly successful, particularly not in the tropical region. Based on the different characteristics of the schemes and their varying performances in different cases, we make recommendations on AR for scatterometer data in order to improve its success rate.

INTRODUCTION

Retrieved scatterometer winds are generally ambiguous (Stoffelen, 1998) and several schemes have been proposed in the past for ambiguity removal (AR). In this paper we present and compare some schemes that were developed for the European Space Agency's remote-sensing satellite (ERS) scatterometer. In addition to the subjective comparison of AR schemes, we present a method for the objective comparison of AR performance among the different schemes. We show that this way of comparison is effective to evaluate the shortcomings of AR schemes, but also reveals a more general way forward to improve AR.

ERS scatterometer winds have a dual ambiguity and there are two wind solutions in each wind vector cell (WVC) on the earth's surface. Several ambiguity removal schemes were evaluated before the launch of ERS-1 [*Graham et al*., 1989], and a scheme called CREO [*Cavanié and Lecomte*, 1987] was selected and implemented by the European Space Agency (ESA). In this scheme two anti-parallel fields from the two solutions at each node are built up. For each field the number of cases in which the highest-probability solution is chosen is calculated. When this number is significantly higher for one of the fields than for the other, then the field with the higher number is selected. This application of CREO is called 'autonomous' ambiguity removal. Using ERS data *Stoffelen and Anderson* [1995] have shown that the probability of the two wind vector solutions is close to 50% and that the rank of the correct solution is spatially correlated, which implies that autonomous ambiguity removal is not likely to be very successful; a conclusion that indeed was found to be true.

If autonomous ambiguity removal fails, or is not applied, then a comparison is made between both anti-parallel wind fields and a numerical weather prediction (NWP) forecast of the surface wind field; the wind field with the higher correlation is selected. Now cases of failure tend to be associated with rapidly changing and/or complex synoptic situations, for which correct scatterometer winds would have been especially valuable. Consequently we developed a procedure to use a short-range NWP forecast to select direction at every node, and introduced a revised ambiguity removal procedure within the PreScat package (*Stoffelen and Anderson*, 1997). This alternative scheme based on the United Kingdom Meteorological

Office (UKMO) scheme SLICE [*Offiler*, 1987], shortly called PreScat here, which improves the ambiguity removal skill.

In all AR schemes considered in this paper, first a local selection of direction is made by choosing the retrieved solution closest to a NWP background wind direction. Experience has shown that the field so produced is reasonable most of the time but there are local regions, i.e., in about 5% of cases, where the solution appears unmeteorological. It is therefore advisable to apply a spatial filter in an attempt to increase meteorological consistency. Besides the purely statistical AR schemes mentioned above, other schemes have been proposed that exploit meteorological balance constraints on convergence and flow rotation. In the following subsections we present the various AR schemes that we mutually compare.

Verification of AR schemes has always been subjective. Some schemes can provide solutions that are meteorologically unreasonable, such as without a closed circulation around a tropical cyclone or with opposed directions in an otherwise uniform flow. If meteorological balance is constraint in the AR this test will obviously not present much errors. Moreover, when comparing two different AR schemes, one can subjectively evaluate the differences. However, this can be very difficult; see, e.g., *Stoffelen and Anderson* (1997) figure 3.

In next section we present an objective method to compare AR schemes. It uses in our case a 24-hour forecast as background in the AR and uses a first guess, i.e., a 0-12 hour forecast for the verification. Since the first guess quality is much better than the background quality in terms of ambiguity selection, the AR skill can be evaluated. Moreover, since often a 24-hour forecast is used for routine AR in operations, it is a very relevant test.

The data used and comparison results are described in subsequent sections, leading to the conclusions and recommendations, where a way forward in AR is suggested by taking advantage of the merits of the different schemes in the different meteorological regions.

PRESCAT

The filter consists of a 5×5 box which slides over the wind field, up to 114 rows at a time. The box first slides in the direction opposite to that of the satellite, starting at the inside edge of the swath and proceeding as in Figure 1a. When it reaches the end of the sector, the direction is reversed, and it exactly retraces its track. On the third pass it starts at the outside edge of the swath and proceeds as in Figure 1b. On the fourth pass it exactly reverses the trace of the third pass.

Within a 5×5 box, the direction at the centre of the box is chosen, based on a weighted average of the differences from the N surrounding points, of which there are usually 24; but there may be less near the edge of the swath if part of the box is over land, or, if some points have been rejected by the quality control on the backscatter measurements [*Stoffelen*, 1998]. At the central point, a mean likelihood, L_i, is calculated for each solution i where

$$L_i = \frac{\sum_{j=1}^{N} C_j \exp[-0.5\{(u_i - u_j)^2 + (v_i - v_j)^2\} q^{-2}]}{N} \qquad (1)$$

and the summation on j is over the N surrounding points in the box. The solution, i, with the highest probability L_i is then selected. The parameter q^2 should represent the wind component variability within a box. Currently a value of q = 2.5 m s^{-1} is used. The computed likelihood of a solution thus depends on the wind vector since speed as much as direction indicates the consistency between neighbouring points.

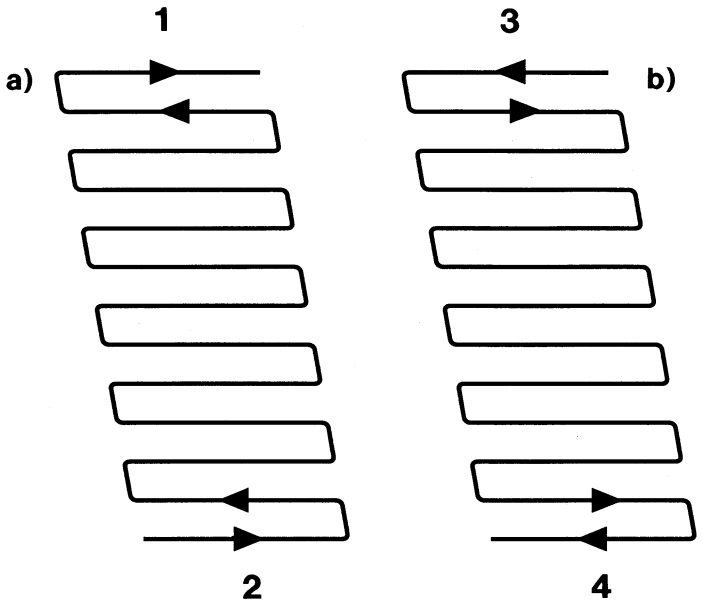

Figure 1. Schematic of the way that the PreScat AR filter slides along an ascending orbit in (a) the first two iterations and (b) the second two iterations.

The parameter C_j represents the confidence in the solution at WVC j. The initial value of C is

$$C = \frac{P \times A \times NN}{4} \tag{2}$$

where P is the scaled probability that the wind direction is within, say, 5° of the true direction, A is the probability that the current solution is the correct one, and NN is the number of nearest neighbours [*Stoffelen and Anderson*, 1995]. Points for which C is low are given low weight, and will not have a strong influence on the selection of a solution at neighbouring points; the opposite is true for points for which $C \approx 1$. Thus, the filter propagates information with high confidence to areas where confidence is low.

The confidence of a point is updated after a pass of the filter according to

$$C = C + (1 - C)L$$

where L is defined in Eq. (1), i.e., confidence is increased relatively mostly when the wind vector at the neighbouring points is consistent, and when we have confidence in the neighbouring solutions (see, eg., Eq. (1)). *Stoffelen and Anderson* [1995] have given the description of a consistency check of the three radar measurements at each location whereby anomalous triplets are rejected (1–2%); these are usually in areas with high variability (i.e., fronts, cyclones, etc.). Because the background information is usually also of lower quality in such areas, and because rejection is often associated with wind shifts, the quality control (QC) benefits the ambiguity removal. *Stoffelen and Anderson* [1995] give a few examples of PreScat AR to both show its strength and weaknesses in important meteorological situations.

VARSCAT

The heuristic VARSCAT algorithm was developed specifically to process the scatterometer measurements (Roquet and Ratier, 1986; Leru, 1999), to improve the operational scheme used at IFREMER (Quilfen and Cavanié, 1991). It is a global procedure minimizing a cost function over the sensor swath corresponding to its full width and to an adjustable length along the satellite track. For this work on the ERS instruments, this

parameter has been set to a maximum of 5,000 km. Given the 25 km grid resolution of the ERS products, it means that the cost function is minimized for an ensemble of 3610 data points. The discretised cost function is defined as follows:

$$J = a\ F_{sig} + b\ F_{ani} + g\ F_{lis} + d\ F_{div}$$

with:

$$F_{sig} = \sum_{ian=1}^{3}\sum_{i=1}^{nbp}\left[s^{\,\mathrm{mod}}_{i,ian} - s^{\,obs}_{i,ian}\right]^2 / \left[Kp_{i,ian}\, s^{\,obs}_{i,ian}\right]^2$$

where *i* and *ian* are the indexes for the point in the swath and the antenna, respectively; *nbp* the number of points considered (maximum of 3610); $s^{\,\mathrm{mod}}$ and $s^{\,obs}$ the normalized radar cross-section (NRCS) derived from CMOD4 and measured by the scatterometer, respectively.

$$F_{ani} = \sum_{i=1}^{nbp}\left[\left(s^{\,obs}_{i,1} - s^{\,obs}_{i,3}\right)/\left(s^{\,obs}_{i,1} + s^{\,obs}_{i,3}\right) - \left(s^{\,\mathrm{mod}}_{i,1} - s^{\,\mathrm{mod}}_{i,3}\right)/\left(s^{\,\mathrm{mod}}_{i,1} + s^{\,\mathrm{mod}}_{i,3}\right)\right]^2$$

where *1* and *3* are the indexes of the fore and aft antennas respecticely.

$$F_{lis} = \sum_{i=1}^{nbp}\sum_{k}\left[v_i \times \sin\left(\Phi_i/2 - \Phi_k/2\right)\right]^2$$

where *v* and Φ are the wind speed and direction, respectively; *k* is the index for the four points (or less near the swath edges) the closest to the point of index *i.*

$$F_{div} = \sum_{i=1}^{nbp}\left[div(\vec{v}_i)\right]^2$$

where $\vec{v}_i$ is the wind vector at point *i* and *div* is the divergence operator. a, b, g, d are empirically-determined weight constants.

Therefore, the cost function contains two smoothness terms, F_{lis} and F_{div}, and two terms to ensure the proximity of the solution to the observed NRCS field, F_{sig} and F_{ani}. Because the relative influence of each term becomes less identifiable as the number of terms of the cost function increases, the minimization is done in two steps. In the first step only F_{sig} and F_{lis} are activated. The latter term avoids large differences in the wind direction at nearby points, its value being maximum for a difference of 180°, and it is weighted by the wind speed to enable a larger wind direction variability at low winds. This step must ensure spatial consistency of the global solution. In the second step are activated the terms F_{sig}, F_{div} and F_{ani}. The latter, called the anisotropy term, is closely related to the wind direction harmonics since the NRCS difference between the two lateral antennas by approximation filters the wind speed NRCS dependency. This term is given a large weight to make more efficient retrieval of the wind direction, the divergence term ensuring the dynamical consistency of the wind field.

2D-VAR

In line with Lorenc (1988), in 2D-VAR ambiguity removal is formulated as a minimisation problem of the objective function:

$$J = J_b + J_o^{scat}$$

where J_o is the observation cost function and J_b the background field cost term. 2D-VAR is based on the analysis of wind increments with the control variable defined as

$$d\underline{x} = (\underline{x} - \underline{x}_b) = \begin{pmatrix} u \\ v \end{pmatrix}$$

where $\underline{x}$ is the control state, $\underline{x}_b$ is the background state, u the west-to-east component of the wind, v and the south-to-north component.

The background term J_b in the cost function is based on a maximum probability formulation and the assumption that errors in the background field have a statistical distribution, which is Gaussian around the wind vector components. The background term quantifies the spatial context of background field errors and determines the spreading of observational information. It is expressed as

$$J_b = d\underline{x}^T B^{-1} d\underline{x}$$

The background error covariances are assumed homogenous and isotropic, i.e., a function of separation distance only (Daley, ….; see figure 2). At each iteration of the minimisation the increments of the control variable are expressed in terms of the spatial structure of the error covariances. As such, these represent the spatial filtering characteristics of 2D-VAR.

The control variable is defined on a so-called “extended grid” (see figure 3) to constrain the analysis to be close to the prior background information outside the swath. Since the analysis is forced to be plausible outside the swath, using this constraint limits overfitting of the scatterometer winds within the swath.

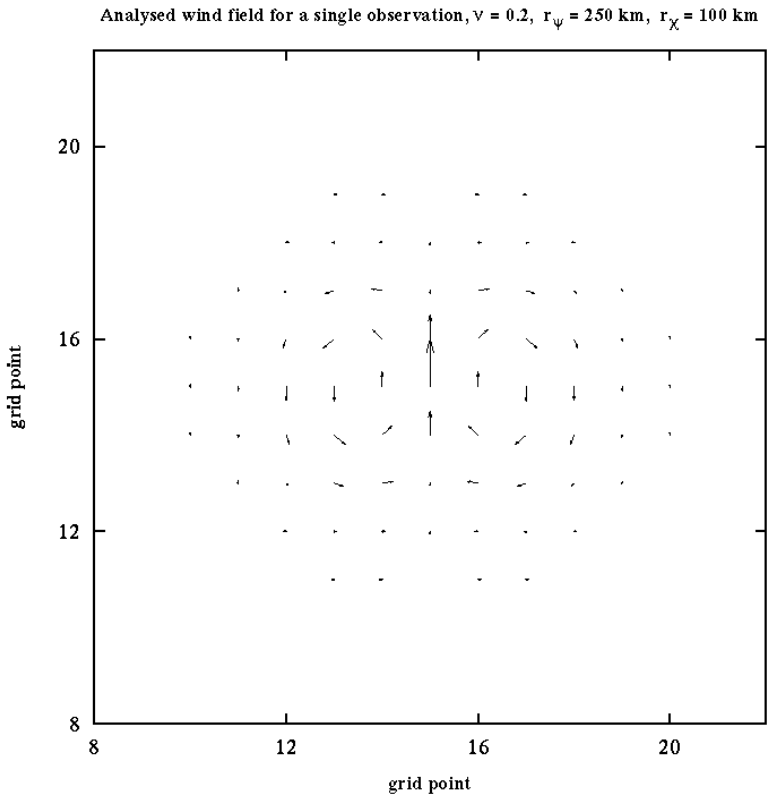

Figure.2 *Wind structure function for the longitudinal (vertical) and transverse (horizsontal) wind error component.*

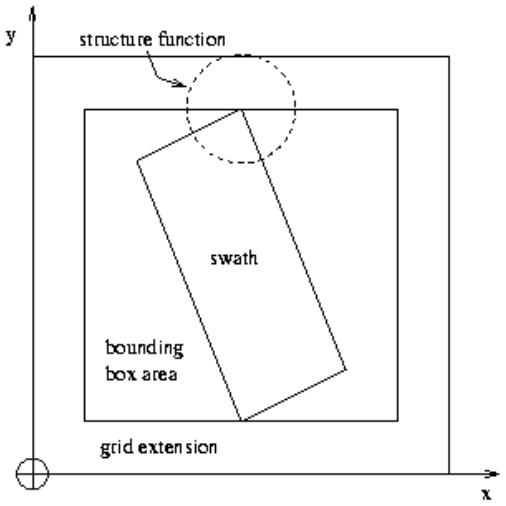

Figure.3 *The extended grid constructed around the bounding box that holds the observations*

The observational term in the cost function J_o^{SCAT} at each WVC is

$$J_o^{SCAT} = \left[\sum_{i=1}^{N} J_i^{-p} \right]^{-1/p}$$

with p = 4 and

$$J_i = -2 \ln P\left(\mathbf{V}^i \middle| d\underline{\mathbf{x}}\right) = \frac{(H(u)-u_i)^2 + (H(v)-v_i)^2}{e_{si}^2} - 2 \ln P_i$$

where $\mathbf{V}^i$ is a wind vector solution, u_i, v_i are the (observation-minus-background) wind component increments, H is an interpolation operator that maps the control variables onto the observations and e_{si} is the standard deviation of the expected total mean component wind error for scatterometer winds that is defined by $e_{si} = 1.8$ m/s. $P_i = 0.5$ for ERS scatterometer winds, since both solutions have (almost) equal probability [Stoffelen, 1998]. After minimisation the analysis is obtained from

$$\underline{x}_a = \underline{x}_b + d\underline{x}_a$$

which constitutes the best estimate for the surface wind field given the background field, the observations, and the objective function. The scatterometer wind solution closest to the analysis is taken to be selected by 2D-VAR.

SCAR

The successive corrections AR (SCAR) as developed by DNMI acts much like 2D-VAR. Its objective function is similar to the one of 2D-VAR, but its principle difference lies in the method of iteration. Variational methods like 2D-VAR perform the minimisation of the objective function in spectral space and as such tend to optimise all spatial scales simultaneously. Successive correction methods on the other hand, tend to first fit the large scales and subsequently fit the smaller ones. This may have an effect on the results.

Another difference with 2D-VAR lies in the fact that SCAR is not using an extended grid, and as such there is no constraint that the analysis should be close to the background information in the extension zone.

METHOD OF COMPARISON

All schemes use a background wind field (BG) in one way or another

- In PreScat and VARSCAT for initialisation of the AR scheme; and
- 2D-VAR and SCAR as a constraint in the objective function.

In the practise of near-real time processing the available global BG is often a 36 hour forecast, which is of poorer quality than an analysis or so-called first guess (0-12 hour forecast) as for example depicted in figure V-13 of Stoffelen (1998). Nevertheless, we find that a 36-hour forecast is generally capable of resolving 97% of the ambiguities in the ERS scatterometer data. Obviously, and as we will see, the remaining 3% of points where the selection (and thus BG wind) is wrong usually coincides with low wind areas or areas with considerable atmospheric dynamics. In particular the latter areas are of great meteorological interest and correct observations in such areas would be particularly useful. Moreover, BG selection errors tend to be spatially correlated and appear in groups of WVCs of varying size.

AR seeks to correct these 3% of wrong selections and in off-line testing and comparing AR schemes we can use a first guess wind field (FG) for verification. Later on we will show that the ECMWF FG on its own probably only provides a wrong selection in less then 1% of cases for ERS scatterometer data. These errors tend to be in the same regions as the BG selection errors, but are generally not correlated otherwise. This can be understood, since

substantial amounts of new additional observations are used to produce the FG, which were not available at the time of production of the 36-hour forecast. The remaining FG errors thus tend to be independent of the BG errors. As such, we can verify most (over 2%) of the corrections of the AR schemes by comparison to a FG.

Our method thus consists in using a BG in the AR scheme application and a FG for performance analysis. For reference we add the BG and FG selections to our data base; all AR schemes should verify better with the FG selection than the BG does. One of the two ambiguities is selected when its vector difference with the reference is smallest. Besides selection statistics, which do not indicate the meteorological gravity of a selection error, we also compute vector RMS difference statistics. In this case, a 180 degree selection error at high wind speed is penalised relatively severely as compared to such error at low wind speed.

DATA

For the AR scheme comparison in this paper about a month of ERS-2 scatterometer retrieved winds are used from January 2000. A typical 12-hourly data coverage plot is shown in figure 4. The ERS-1 was launched on 17 July 1991, carrying a C-band scatterometer. The satellite flies in a polar orbit at a height of 800 km. The scatterometer instrument, which is also mounted on ERS-2 launched in 1995, has three independent antennae pointing in a horizontal plane towards a direction of 45°, 90°, and 135° with respect to the satellite propagation, thus illuminating a site in the scatterometer's swath three times, by the fore, mid, and aft beam, respectively. The incidence angle of the radar beam varies from 18° to 47° for the mid beam, and from 24° to 57° for the fore and aft beams. The swath, approximately 500 km wide, is sampled every 25 km resulting in 19 measurement nodes across the swath; along the swath the sampling distance is also equal to 25 km. The nodes are not independent, however, and the effective spatial resolution of the instrument on the earth's surface (called the footprint) is approximately 50 km. A quality control procedure is implemented which identifies and rejects 1-2% anomalous triplets of backscatter measurements [*Stoffelen*, 1998].

Since AR schemes act as spatial filters, the way of presentation of consecutive WVCs to these schemes is relevant. The schemes can only constrain spatial consistency over a certain domain. One orbit constitutes about 1,600 WVC rows, and ~800 WVC rows exist from pole to pole. PreScat is able to process from pole to pole and thus processes all continuous pieces of ocean swath in one batch. 2D-VAR, VARSCAT, and SCAR all process about 200 WVC rows in one batch. We checked the continuity between batches and found generally no problem with continuity. In the few January cases where a discontinuity is present over the swath due to the batches, it was not clear whether the situation improves when processed in a single batch (not shown). In general, we believe that the splitting up in batches does not affect our results seriously.

The BG wind field used for the four AR schemes is retrieved from ECMWF. For observation times of

- $12h < t \leq 24h$ a BG from forecasts with lead time from 24 to 36 hours at 6-hourly intervals is used; and
- $0h < t \leq 12h$ a BG from forecasts with lead time from 36 to 48 hours at 6-hourly intervals is used,

i.e., once a day at verification time noon a move is made to the next day forecast and forecast lead drops from 48 hours to 24 hours. This "day break" was not found to cause any problem in the AR.

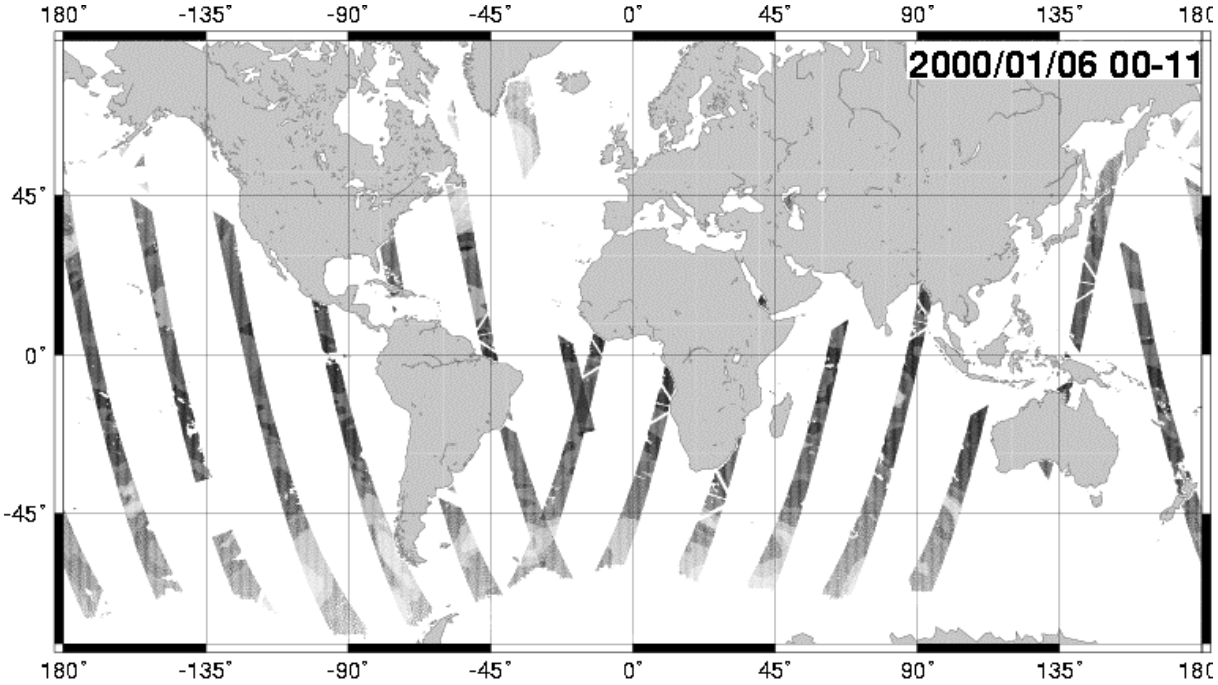

Figure4. *12-hourly wind coverage plot centred around 6 UTC 6 January 2000. Grey shades over sea depict ERS scatterometer wind speed*

The FG at appropriate time is used for verification. This is a cubic time interpolation between a 3-, 6-, and 9-hour forecast to the actual observation time. These ECMWF fields are available from the 0, 6, 12, and 18 UTC forecasts in January 2000.

COMPARISON RESULTS

STATISTICAL RESULTS

Activity and performance of the AR schemes were investigated for all wind speeds. However, as expected, for winds below 3 m/s the activity is large and the performance low for all schemes. As such, we did not further statistically investigate winds below 3 m/s.

ACTIVITY

Figure 5 shows histograms of the scores of the different AR schemes. In the black rightmost column the percentage of selections differences between BG and FG is shown, which varies between 1-6%. The activity of an AR scheme may be measured by adding the light and dark grey columns, since this represents the percentage of difference of selections with respect to the BG. Doing so, we note that the AR schemes generally do not have the level of activity necessary to correct all BG selection errors and room for improvement probably remains.

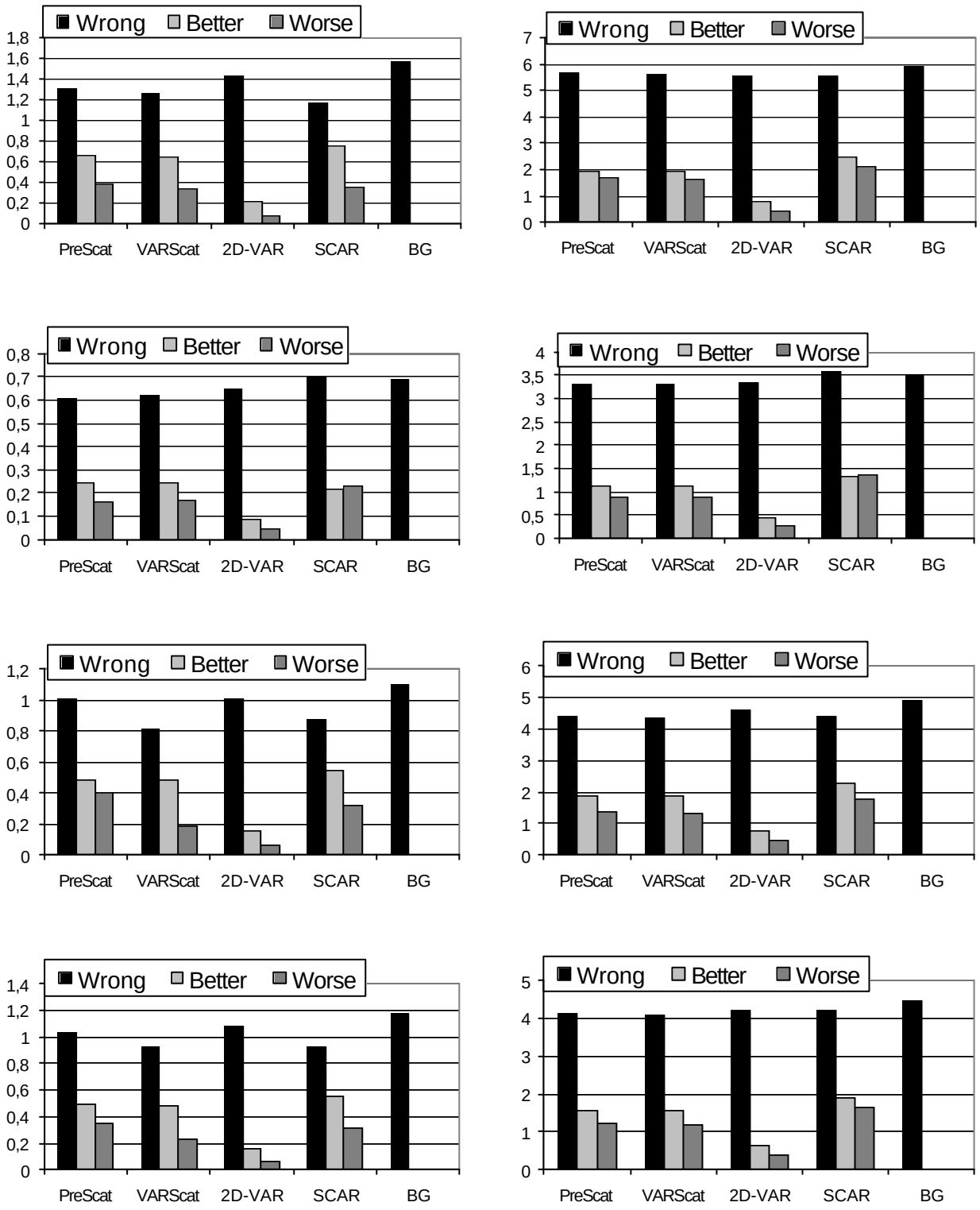

Figure 5. *Percentage AR scores. In each panel the rightmost column is the percentage of BG selections different from the FG selections. The light grey column is the percentage of selections where the AR scheme solution is in line with the FG selection, but not with the BG selection. The dark grey column presents the percentage of cases in which the AR scheme disagrees with both FG and BG. Right panels represent wind speeds between 3 and 7 m/s, left panels winds above 7 m/s. From top row to bottom, respectively the NH, tropics, SH, and all results together are shown.*

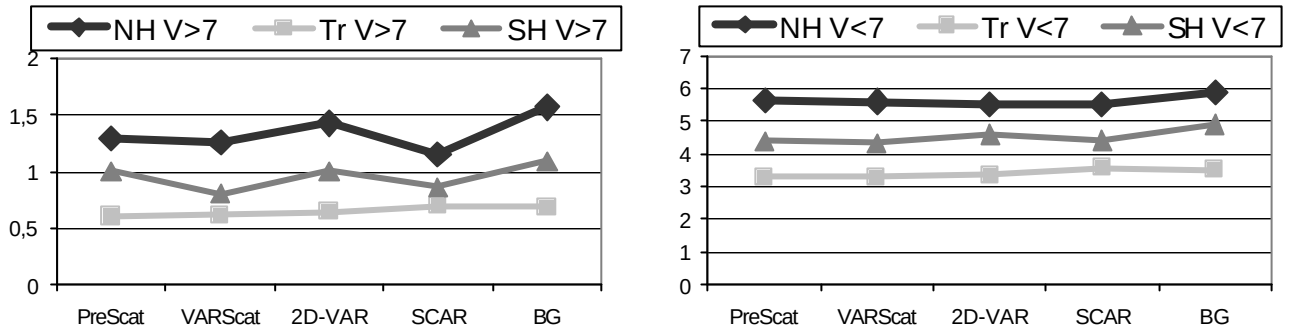

Figure 6. *Percentage of difference with FG versus AR scheme for wind speeds above 7 m/s (left) and for wind speeds 3-7 m/s (right).*

The level of activity of 2D-VAR is clearly below that of all other AR schemes, whereas SCAR appears generally as the most active. There are also geographical differences; in the tropical region (below 20 degrees latitude) the discrepancy between BG and FG is relatively small and in line with this the activity of the AR schemes is lowest here, albeit far too low to correct all wrong BG selections. The relatively good scores in the tropics at low winds are probably due to the trade winds.

PERFORMANCE

Ambiguity removal is generally beneficial, since the "better" column in figure 5 is generally taller than the "worse" column. Moreover, activity generally pays off, since the taller the grey columns, the larger the difference between "better" and "worse". Figure 6 summarises the selection performance. All this is particularly clear when comparing 2D-VAR to the other AR schemes. We already noted that the activity of 2D-VAR is largely insufficient and therefore one may expect better scores for the more active AR schemes. SCAR is the most active, and this does particularly pay off in the NH and SH at high winds.

In the tropics, the SCAR activity seems to be detrimental as compared to the BG reference. More in general, we note that the difference between the two grey columns in Figure 5 is small compared to their lengths. This indicates that AR schemes appear generally as ineffective. This ineffectiveness seems to depend on AR scheme and geographical region, which gives some scope for improvement, when the physical characteristics of the schemes are compared and the AR schemes are updated. Also, changes at high wind seem more effective on average than AR changes at low wind speeds.

LARGE SCALE ERRORS

In order to better understand the scale of the AR scheme error characteristics, we look into subsequent areas of 19.19 = 361 nodes where more than 72 wind vector selections (> 20%) are different. Subsequently, we checked all WVC in such massages against BG and FG. We comment on some peculiar findings here.

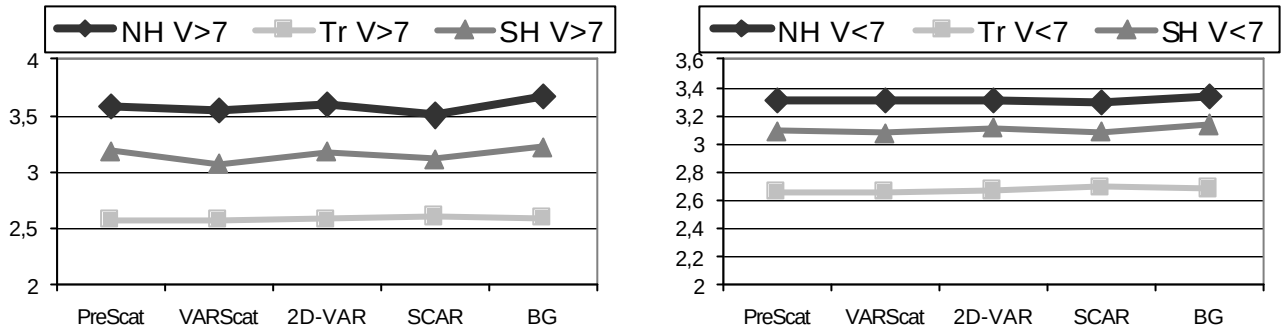

Figure 7. *RMS of wind vector difference of AR scheme with FG versus AR scheme for wind speeds above 7 m/s (left) and for wind speeds 3-7 m/s (right).*

Speed > 7 m/s	NH		Tropics		SH	
	BG	FG	BG	FG	BG	FG
PreScat	89	79	79	87	82	73
SCAR	83	88	73	64	83	83

Table 1. *Percentage of identical selection between AR schemes (rows) and BG and FG fields (columns) in case of large-scale discrepancies (see text) between PreScat and SCAR.*

Table 1 shows results for the different geographical regions for wind speeds above 7 m/s for messages where PreScat and SCAR selections deviate by more than 20%. SCAR shows generally more activity (more different from BG) and clearly a better score in the NH and SH. In the tropics however, the SCAR activity is clearly penalised and PreScat is doing a much better job on the large-scale corrections at high winds. We do not show the results at low winds, since these largely confirm the general statistical results discussed in previous subsection.

Table 2 shows the results for the tropical region for wind speeds above 7 m/s for messages where PreScat and 2D-VAR selections deviate by more than 20%. These cases overlap with the tropical cases shown in table 1, but are 50% less in number. In this case 2D-VAR outperforms PreScat by almost 10%, which is unique. The BG verification suggests that 2D-VAR performs better because it is inactive though. Since both FG scores are not good, it suggests that the cases with 20% difference are due to both poor BG and poor AR (of PreScat).

Speed > 7 m/s	BG	FG
PreScat	66	48
2D-VAR	95	57

Table 2. *As table 1, but between PreScat and 2D-VAR, and for tropical wind selections only.*

PreScat was also compared to VarScat, showing that PreScat slightly better verifies with the FG (except in the SH for wind speeds over 7 m/s where the opposite holds), where the activity of both schemes is similar. Apparently, VarScat is more effective in correcting small scale errors, since its overall performance is generally better.

WIND VECTOR PERFORMANCE

Figure 7 translates the general selection performance as depicted in figure 6 into a wind vector RMS performance. This may be of high meteorological interest since more weight is given to errors as they occur at higher wind speed. However, very similar conclusions may be drawn from figures 6 and 7

- PreScat works best in the tropics, closely followed by VarScat;
- VarScat outperforms in the summer SH and on average everywhere; and
- SCAR is the most beneficial one in the winter NH.

METEOROLOGICAL CASES

In order to understand the statistical results, maps were investigated that show selection differences. Some illustrative cases are shown in Appendix A, where we focus on areas of large discrepancy between the AR schemes. A first and important assessment is that the FG looks generally consistent with one of the two scatterometer solutions, indicating that the FG is indeed a good reference for validation of the AR schemes. As may be expected, the scatterometer shows small-scale information not present in the generally smooth FG.

However, at wind speeds below 5 m/s, usually in the tropical region, the FG flow can be occasionally inconsistent with a flow depicted by either one of the two wind vector solutions (see e.g. Case I App. A). On the other hand, we still believe that the FG is generally useful for wind speeds 3-7 m./s to validate the AR schemes. The performance of all AR schemes at low wind speed thus can be improved in our view, since the scores in figures 6 and 7 are poor as compared to the BG score.

In all cases of large differences between AR schemes, be it low or high wind speed, the BG does verify poorly. Sometimes, some of the AR schemes are able to largely correct the initial BG choice (e.g. PreScat and SCAR in Case I and Case IV of App. A), but at other times the BG initial choice is not corrected. For example, in Case IV of App. A 2D-VAR and VarScat are not able to produce the fairly simple flow pattern because of BG errors. Such dependency on the BG is undesired, particularly in case of subsequent NWP data assimilation.

In the cases presented in App. A we can see effects due to the limited batch size of the SCAR and VarScat AR schemes (Cases I, II, and IV). Since the cases presented are selected cases of particular large discrepancy, these show the gravest batch effect in our data set. Where in some of those cases batch size would have affected the statistical score, the frequency of occurrence of such effects is very low and we believe does not much affect the statistical results.

Case V is very interesting indeed since it illustrates the spatial filtering characteristics of each scheme by looking at the angle and extent over which the errors occur. PreScat shows the smallest error over a small segment of the low and a radial extent of about 300 km. This corresponds to the filter width used in PreScat AR. On the other hand SCAR shows an error in a much larger segment extending to about 500 km in radial direction, corresponding to the rather broad spatial structure functions used.

DISCUSSION AND CONCLUSIONS

An AR scheme comparison has been carried out at KNMI. AR schemes used a 24-36 hour forecast as BG and a FGAT for objective verification. Ambiguity selections based solely on the BG result in generally 3% of error. However, these cases present meteorologically dynamic and thus relevant situations, such as developing waves, and mispositioning of lows and tropical cyclones. For wind speeds below 7 m/s, the number of selection errors is larger than for wind speeds above 7 m/s. On the other hand, the meteorological relevance of selection errors at lower wind speed is smaller indeed. In line with this we excluded selection errors below 3 m/s in our comparisons.

AR schemes are generally only able to bring the BG selection error percentage down to 2% and thus are not very effective in general. Stratified by geographical region and wind speed class, AR scheme scores with respect to the BG vary from slightly detrimental to about 25% beneficial, and based on AR scheme characteristics a number of potential improvements emerge

- The number of selections that is different between BG and AR scheme is denoted activity here. Activity generally pays off, but is penalised in the tropical region; the inactive 2D-VAR only scores well in the tropics and the active SCAR is slightly detrimental here. Activity is controlled by the structure function for 2D-VAR and SCAR; the wider the structure, the broader the spatial scope of changes. Also, the weight of the BG winds in the objective function may be decreased to increase activity. PreScat and VarScat can also be changed to affect activity. Based on our results, tests with varying activity of the AR schemes, are expected to show more optimal performance in particular geographical regions, and location-dependent settings could evolve.
- The fact that PreScat works best in the tropics and SCAR is the most beneficial one in the winter NH appears related to the physical constraint used for AR. PreScat uses wind vector continuity and SCAR uses the constraint that changes with respect to the BG should be rotational rather than divergent (see also figure 2). Such wind structures appear for geostrophically-balanced wind fields. However, the geostrophical balance breaks down in the tropical region and wind vector continuity better characterises the flow here. This is an obvious explanation for our results. The PreScat wind vector continuity constraint may also be used in 2D-VAR and SCAR by using structures of equal rotation and divergence as depicted in Daley (1991). Also in PreScat and VarScat one could vary the constraint with respect to rotation, albeit in a less straightforward way. We thus recommend testing of geographically-dependent structure functions for AR.

AR errors occur in spatially coherent structures. We find that large error structures tend to appear less for PreScat. Given the overall scores, PreScat has relatively frequent small error patches in the SH and NH. Of all schemes 2D-VAR and VARScat seem most dependent on the BG input. The active SCAR is more independent of the BG, but clearly overactive in the tropical region.

In terms of relative performance VARScat outperforms on average, PreScat is generally best in the tropics, SCAR in the winter NH, and VarScat in the summer SH. 2D-VAR should be clearly made more active in general, while the other schemes, as discussed above, probably would benefit from geographically-dependent settings.

In case of large dynamical errors in the BG, FGAT seems to be generally correct. As such we recommend FG for AR in NWP applications where FG information is readily

available. Moreover variational schemes, such as 3D-Var or 4D-Var, are recommended to use FG and multiple ambiguous scatterometer wind solutions in the meteorological analysis objective function (Stoffelen, 2000).

ACKNOWLEDGEMENTS

We acknowledge EUMETSAT for funding the OSI SAF, in which context this work was carried out, and Météo France for hosting it. John de Vries produced figures 2,3, and 8 which we greatly appreciate.

REFERENCES

Cavanié, A. and P. Lecomte, Vol 1 - Study of a method to dealias winds from ERS-1 data. Vol 2 - Wind retrieval and dealiasing subroutines, *ESA contract 6874/87/CP-I(sc) report*, ESA publications division, Noordwijk, the Netherlands, 1987.

Daley, R., Atmospheric data analysis, Cambridge atmosph. and space science series, Cambridge University Press, 1991.

Graham, R., D. Anderson, A. Hollingsworth and H. Böttger, Evaluation of ERS-1 wind extraction and ambiguity removal algorithms: meteorological and statistical evaluation, *ECMWF report*, ECMWF, Reading, England, 1989.

Leru M, 1999: Inversion des mesures radars diffusiomètriques d'ERS-1 et ERS-2: Etude d'une nouvelle approche basée sur une méthode variationnelle. IFREMER technical report, n° 99-05, 71 pp.

Lorenc, A. C., 1988, Optimal nonlinear analysis, Quart. J. Royal Meteor. Soc. **114**, pp. 205-240.

Offiler, D., ERS-1 wind retrieval algorithms, *U. K. Meteorol. O. 19 Branch Memorandum No 86*, Meteorological Office, Bracknell, England, 1987.

Roquet H. and Ratier A., 1988: Towards direct variational assimilationof scatterometer backscatter measurements into numerical weather prediction models. Proc. of Igarss 1988, Edinburgh, Scotland, 257-260.

Stoffelen, A., and D. Anderson, The ECMWF contribution to the characterization, interpretation, calibration and validation of ERS-1 scatterometer backscatter measurements and their use in numerical weather prediction models', *ESA contract 9097/90/NL/BI report*, Eur. Centre for Medium-range Weather Forecasts, Reading, England, 1995.

Techn. Memo 194, ECMWF, Reading, England, 1993.

Quilfen Y. and Cavanié A., 1991: A high precision wind algorithm for the ERS-1 scatterometer and its validation. Proc. of Igarss 1991, Espoo, Finland, 873-876.

APPENDIX A

A selection of cases is given where in a large number of cases two AR schemes differ in wind vector selection. The cases are presented in order of increasing wind speed. First the date and time are indicated for each case, then the two schemes are indicated, the number of differences, lat/lon, and a set of conclusions. The 6 maps depict respectively VARScat, SCAR (DNMI), PreScat, 2D-VAR, BG (ECMWF), and FG (ECMWF_FGAT).

CASE I DATE 2000/01/13 20:47:46

```
Selection:  number prescat <> dnmi
number differ : 270 0.844595  in  3  message(s)
longitude -161.57
latitude   -17.00
```

- Wind speeds < 5 m/s
- DNMI has a message edge effect, but not serious
- Small scale wind flow unclear
- VARSCAT and 2DVAR show internal inconsistency
- BG (+24) incorrect

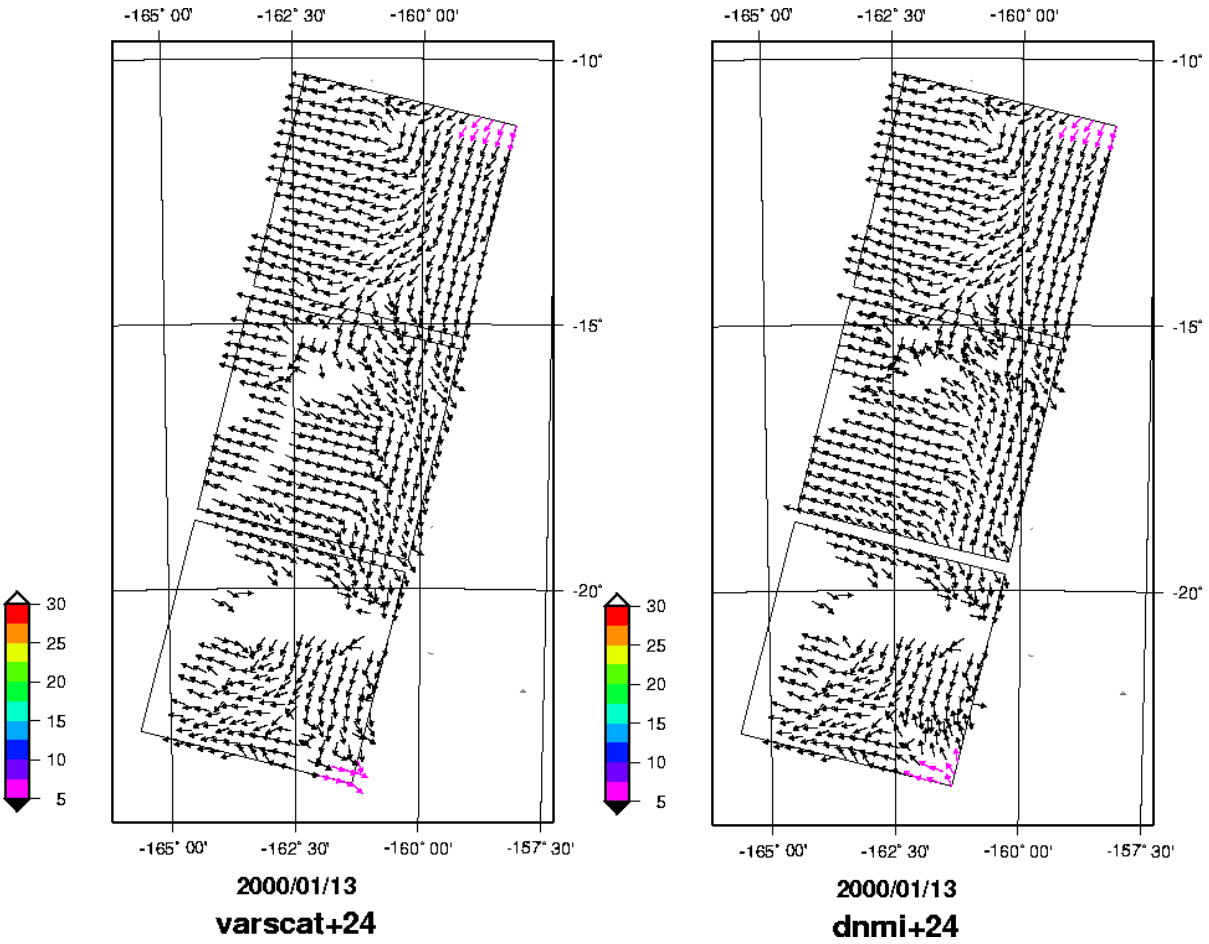

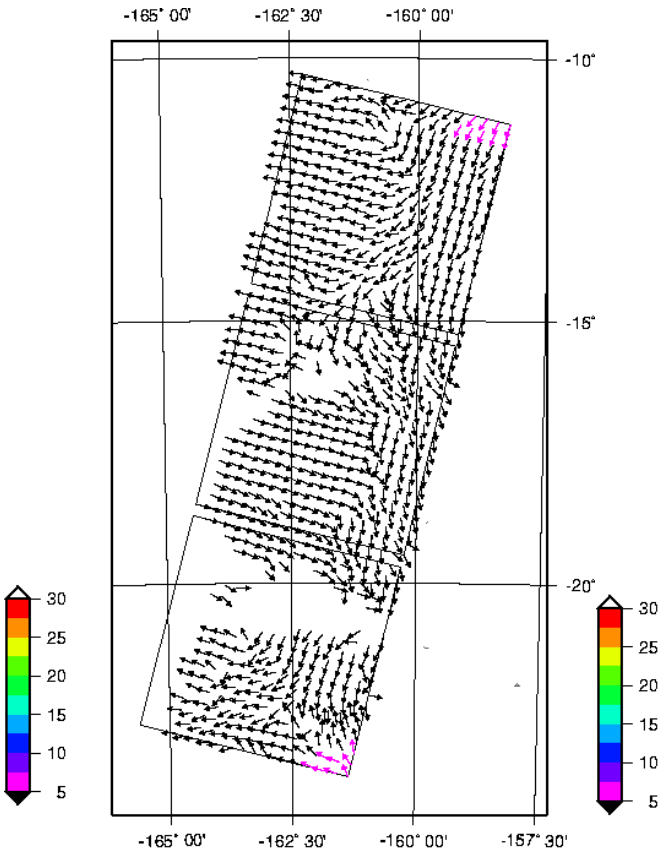

2000/01/13

prescat+24

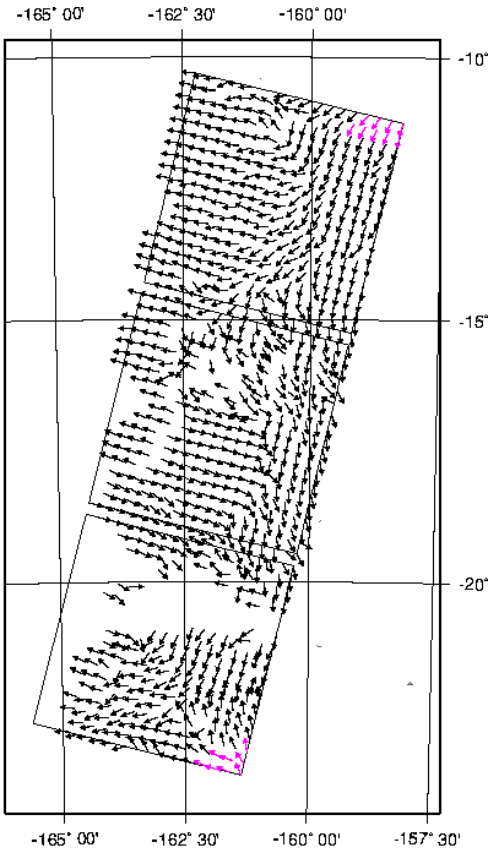

2000/01/13

2dvar+24

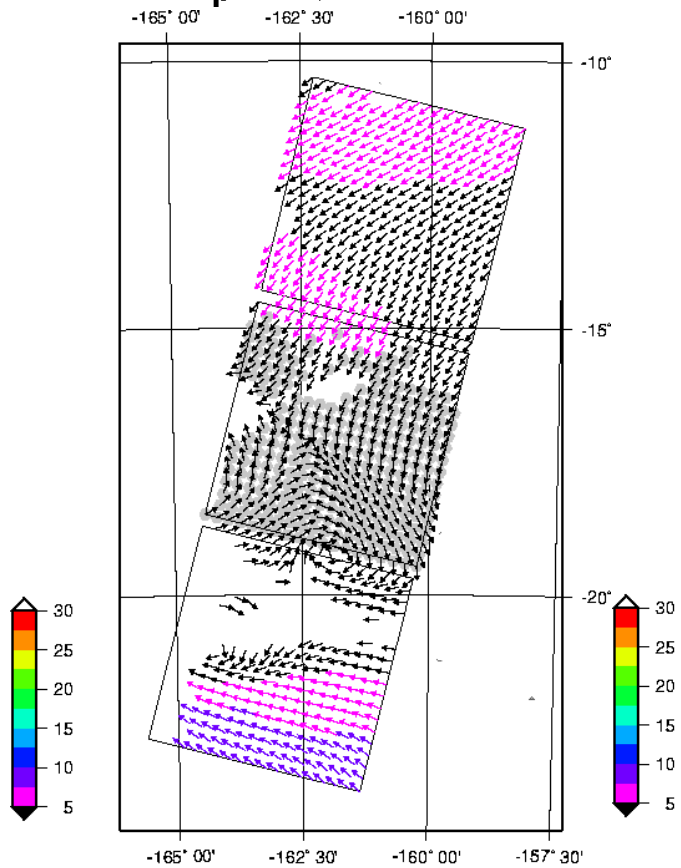

2000/01/13

ECMWF+24

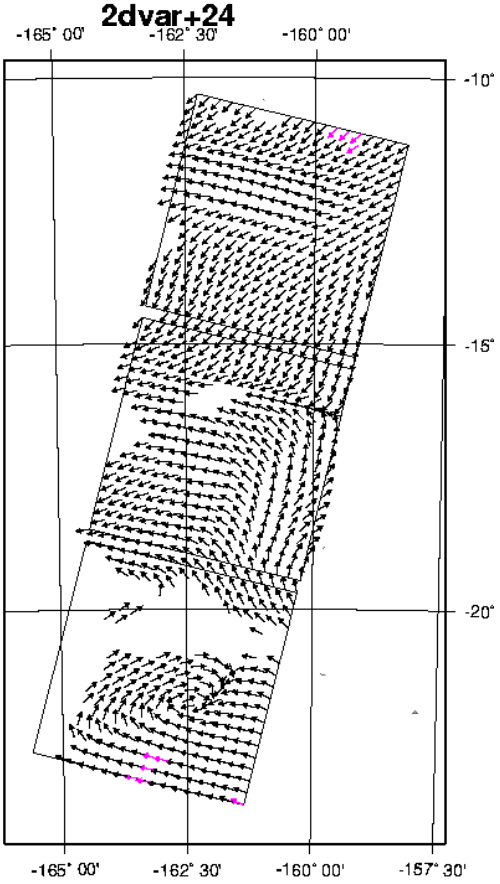

2000/01/13

ECWMF_FGAT

CASE II DATE 2000/01/16 09:49:48

```
Selection:  number prescat <> varscat
number differ : 228 0.727914  in  3  message(s)
longitude -163.49
latitude   -16.20
```

- Wind speeds 0-10 m/s
- Noisy; all AR schemes show inconsistencies of some sort
- VARSCAT shows a major badge edge effect

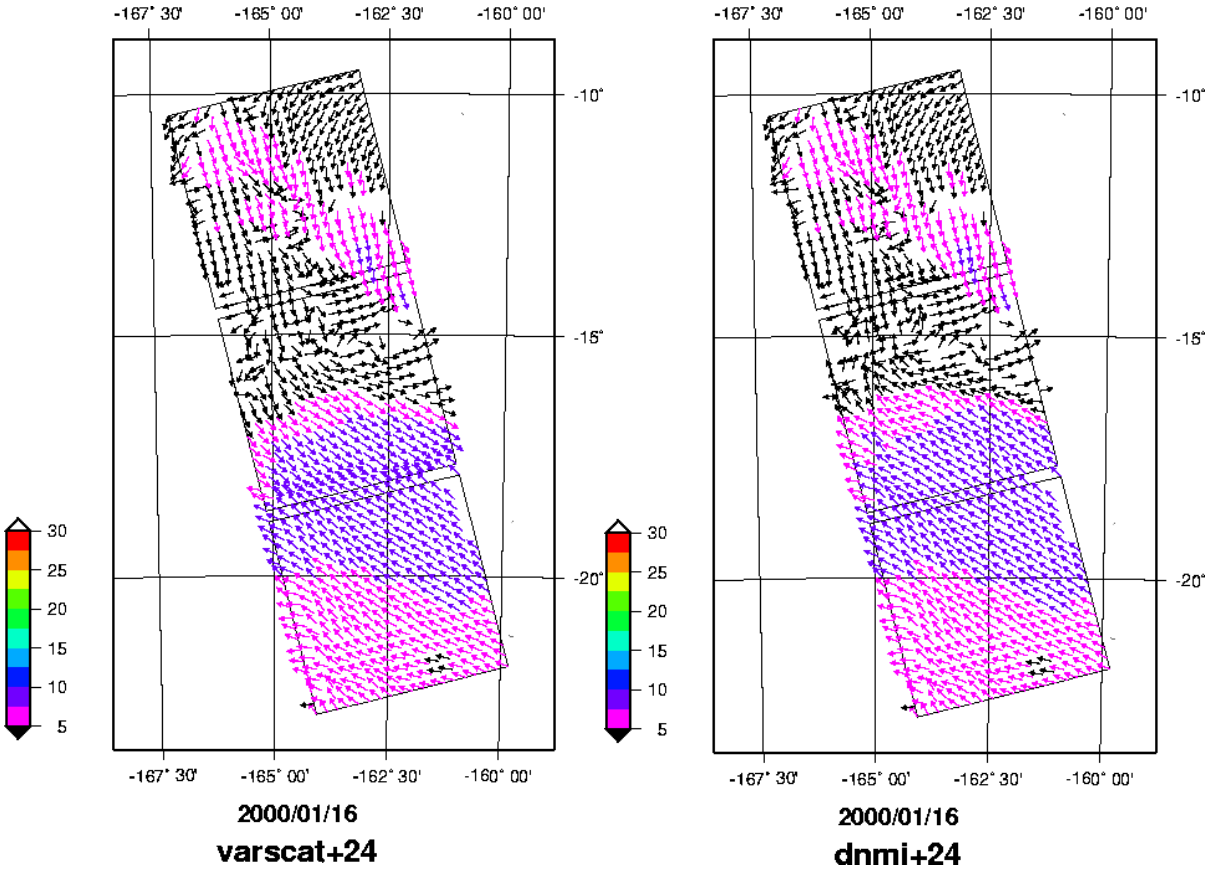

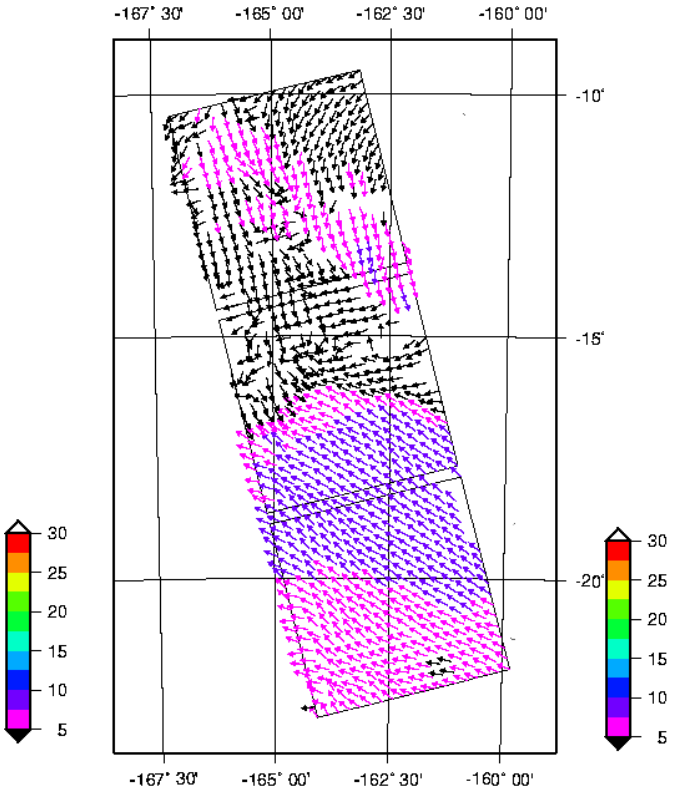

2000/01/16

prescat+24

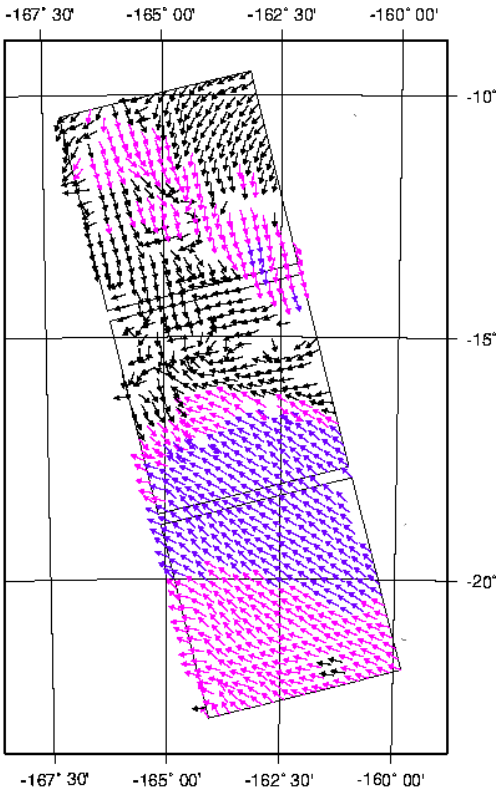

2000/01/16

2dvar+24

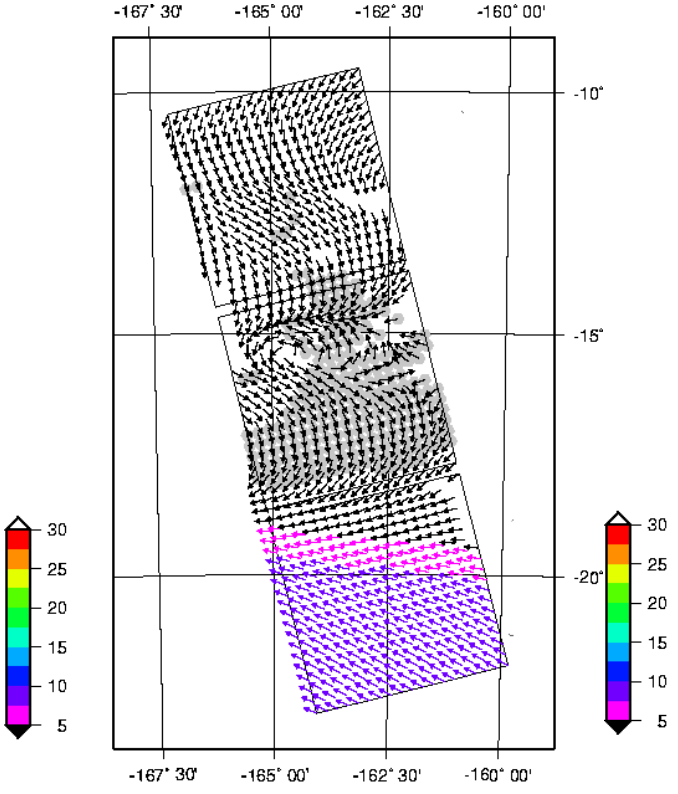

2000/01/16

ECMWF+24

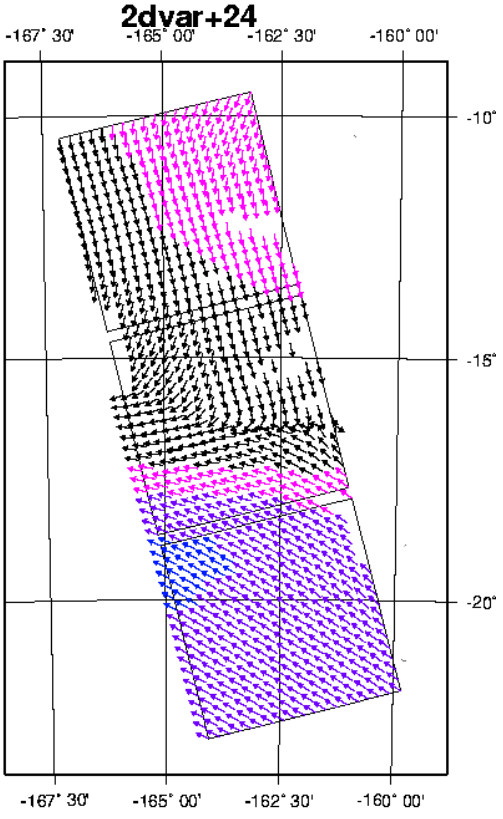

2000/01/16

ECWMF_FGAT

CASE III DATE 2000/01/06 01:35:12

```
Selection:  number prescat <> varscat
number differ : 244 0.741299  in  3  message(s)
longitude  -34.52
latitude   -37.41
```

- Wind speeds 0-10 m/s
- VARSCAT and 2DVAR follow wrong BG
- But PRESCAT and DNMI mostly correct
- BGFG (+24) is incorrect

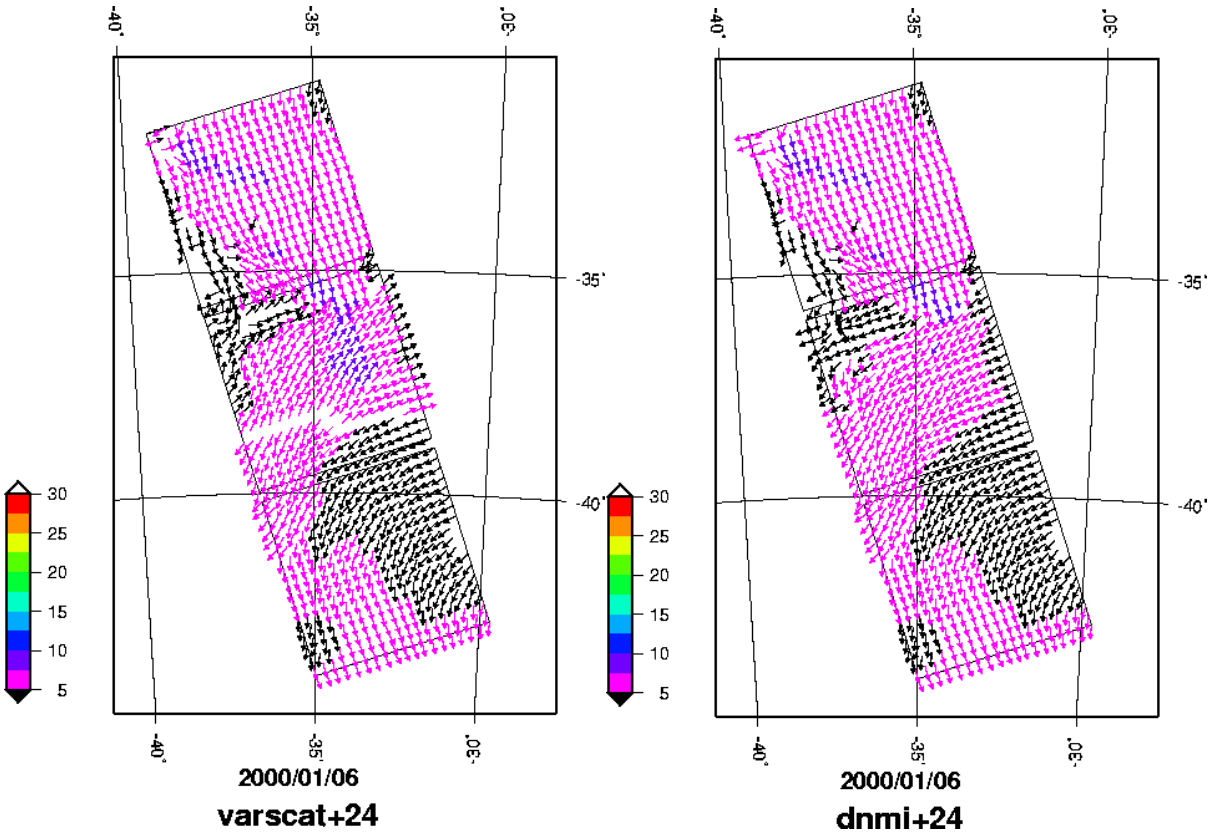

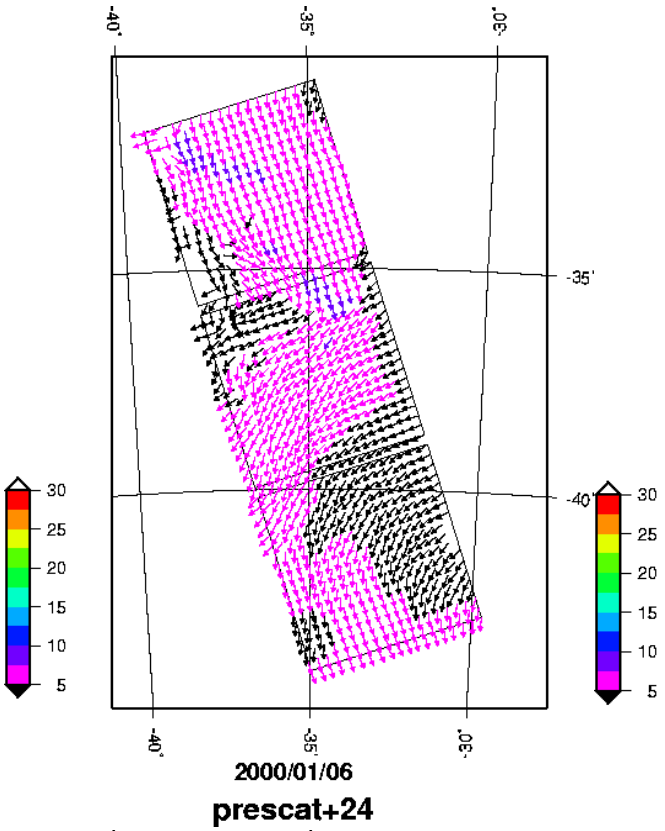
-40°
-35°
-30°
-35°
-40°
30
25
20
15
10
5
2000/01/06
prescat+24

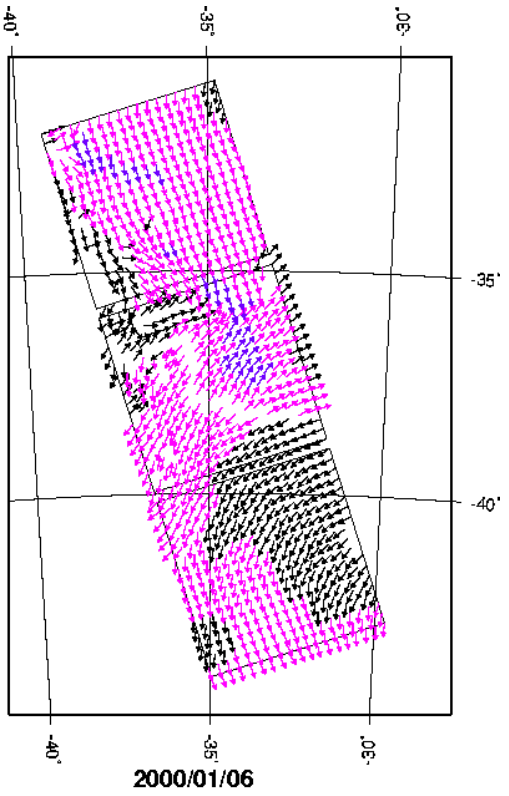
-40°
-35°
-30°
-35°
-40°
2000/01/06
2dvar+24

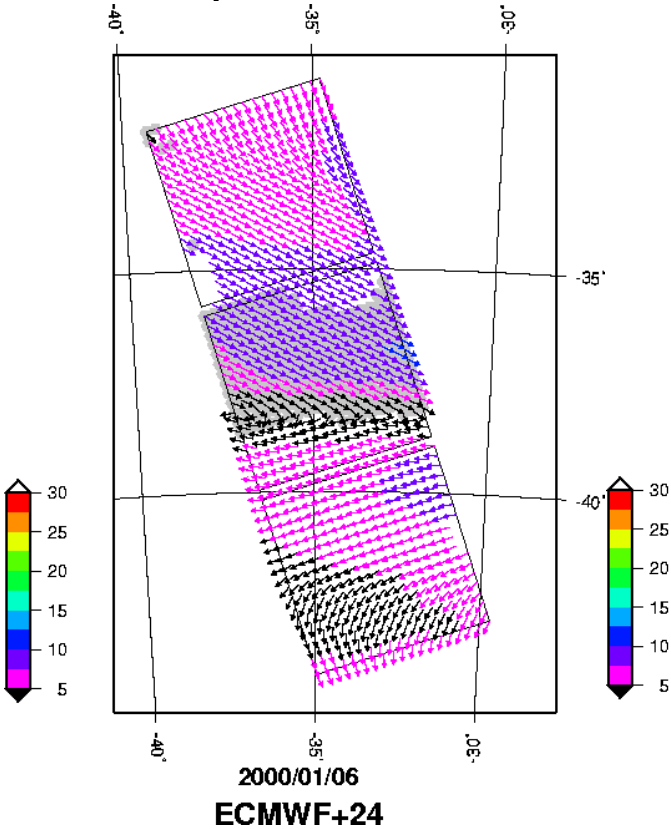
-40°
-35°
-30°
-35°
-40°
30
25
20
15
10
5
2000/01/06
ECMWF+24

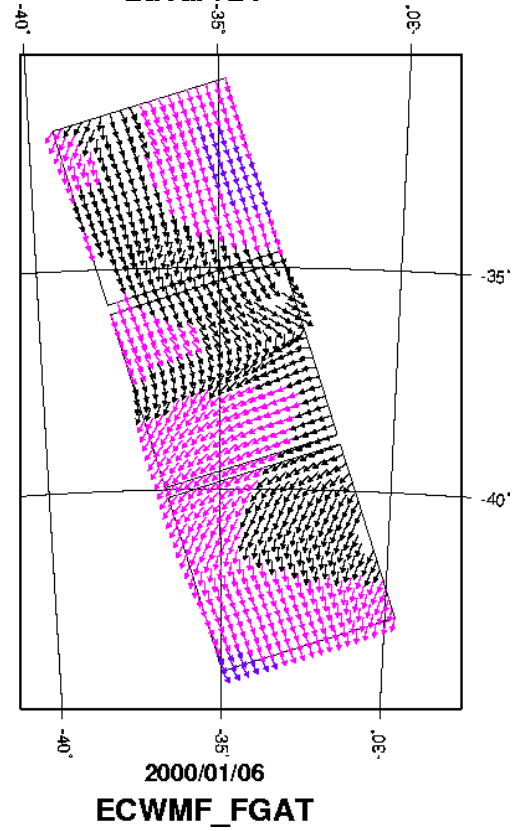
-40°
-35°
-30°
-35°
-40°
2000/01/06
ECWMF_FGAT

CASE IV DATE 2000/01/19 06:20:17

```
Selection:  number prescat <> varscat
number differ : 446 0.755937  in  4  message(s)
longitude  -92.33
latitude   -60.29
```

- wind speeds 5-15 m/s
- BGFG (+24) large dynamical error
- VARSCAT and 2DVAR more or less follow wrong BG
- DNMI corrects half of wrong BG
- DNMI shows badge edge effect
- PRESCAT almost fully corrects wrong BG
- all AR schemes show one or more areas with large inconsistencies

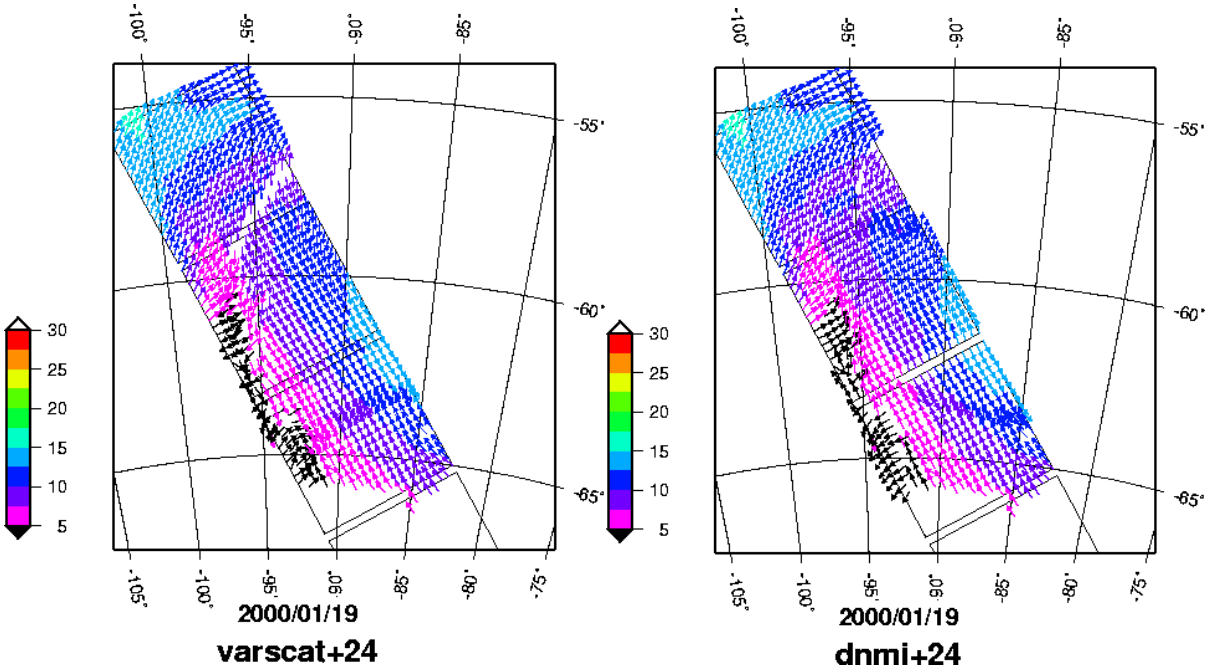

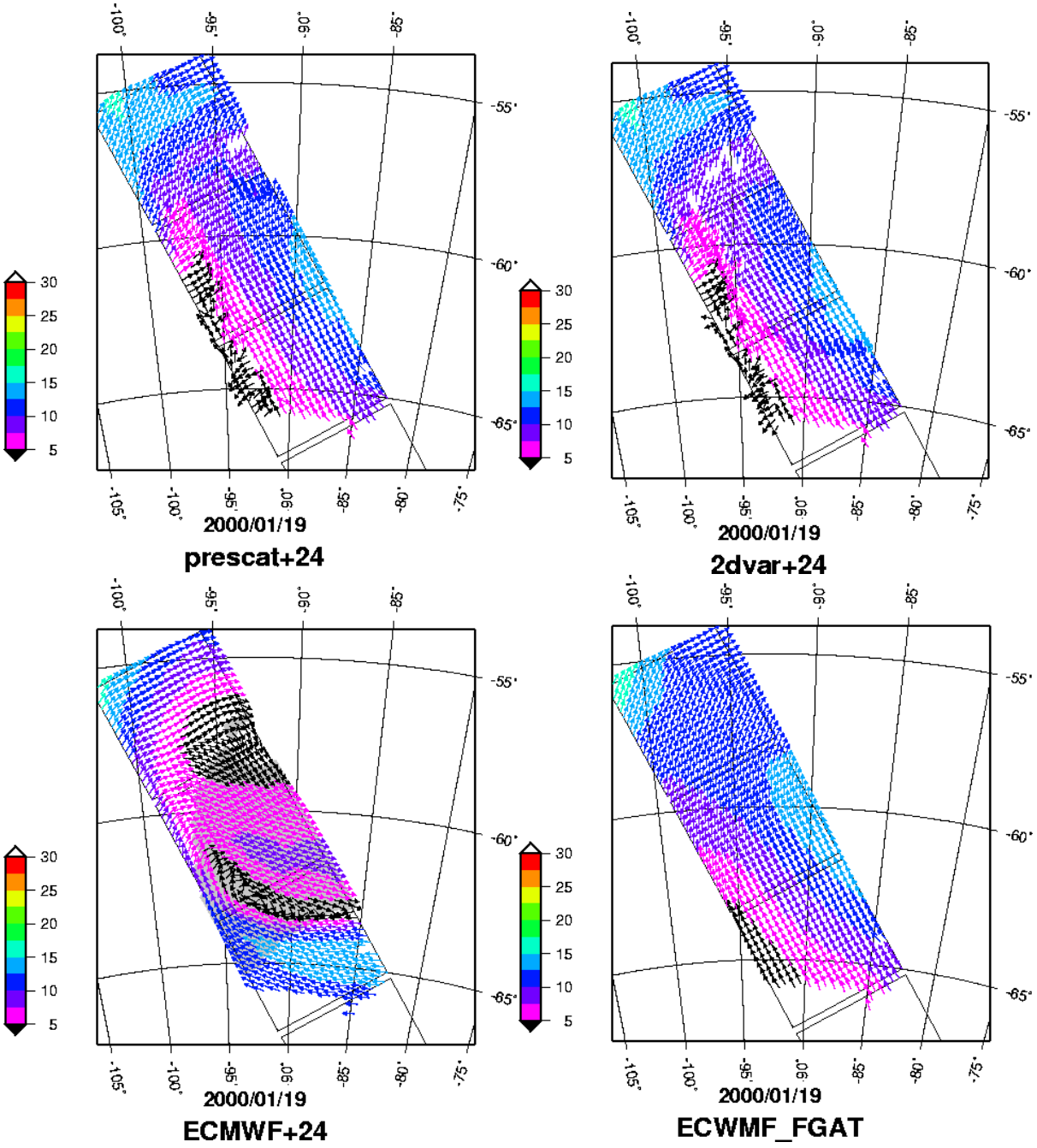
30
25
20
15
10
5
-105°
-100°
-95°
-90°
-85°
-80°
-75°
-55°
-60°
-65°
2000/01/19
prescat+24
2dvar+24
ECMWF+24
ECWMF_FGAT

CASE V DATE 2000/01/31 11:22:37

```
Selection:  number prescat <> dnmi
number differ : 491 0.780973  in  4  message(s)
longitude  -24.72
latitude   -32.97
```

- wind speeds 10-20 m/s
- BG (+24) large dynamical error at high winds
- PRESCAT 1/6 segment error in low segment ; radius 300 km
- VARSCAT ½ segment error in low segment ; large radius 500 km
- 2DVAR 1/3 segment error in low segment ; radius ~350 km
- DNMI 1/3 segment error in low segment ; large radius ~500 km

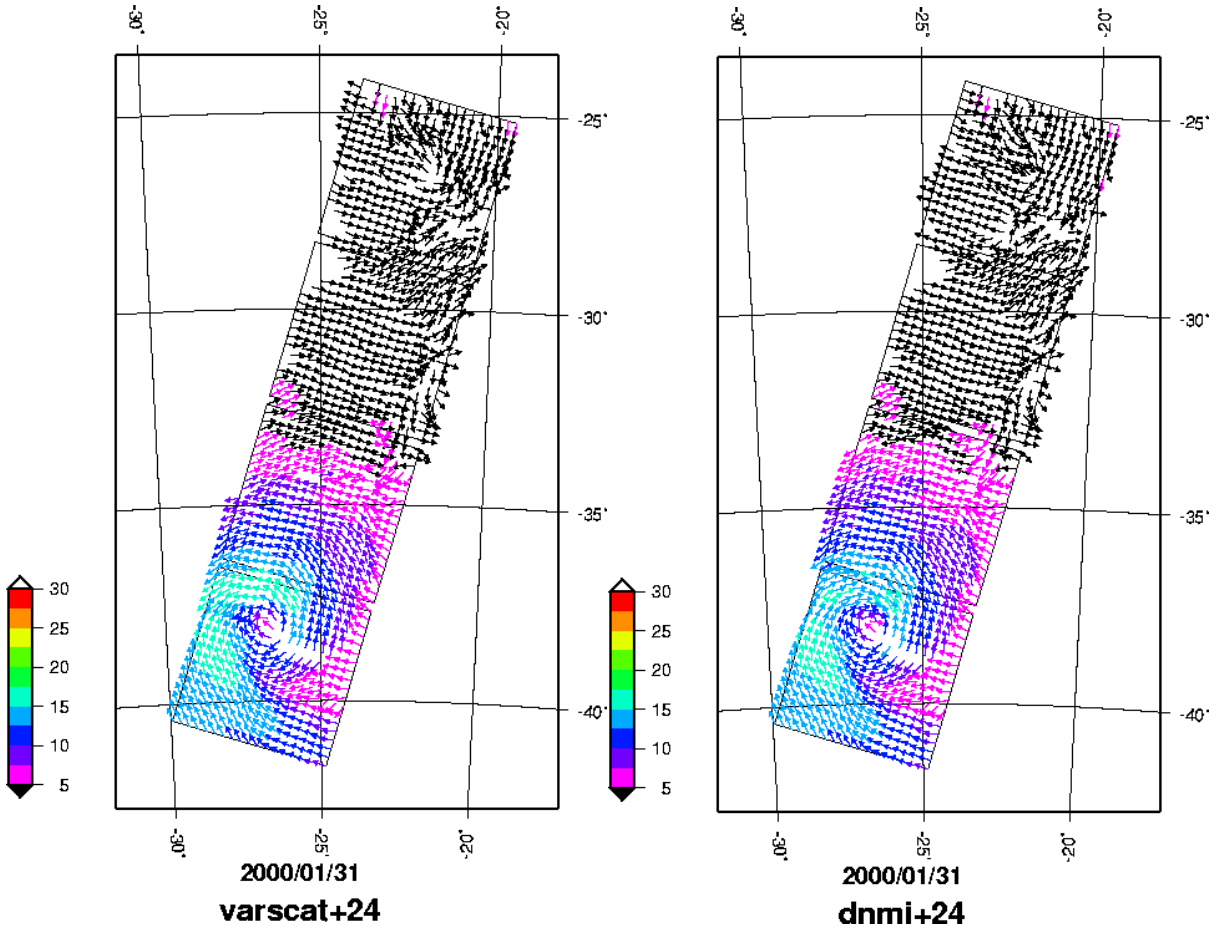

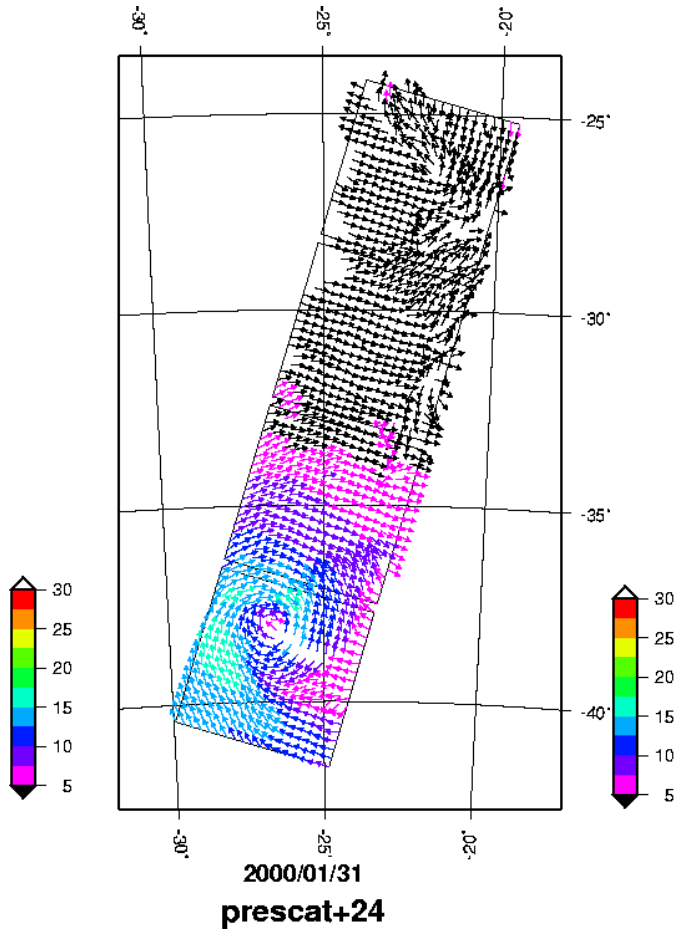
-30°
-25°
-20°
-25°
-30°
-35°
-40°
30
25
20
15
10
5
2000/01/31
prescat+24

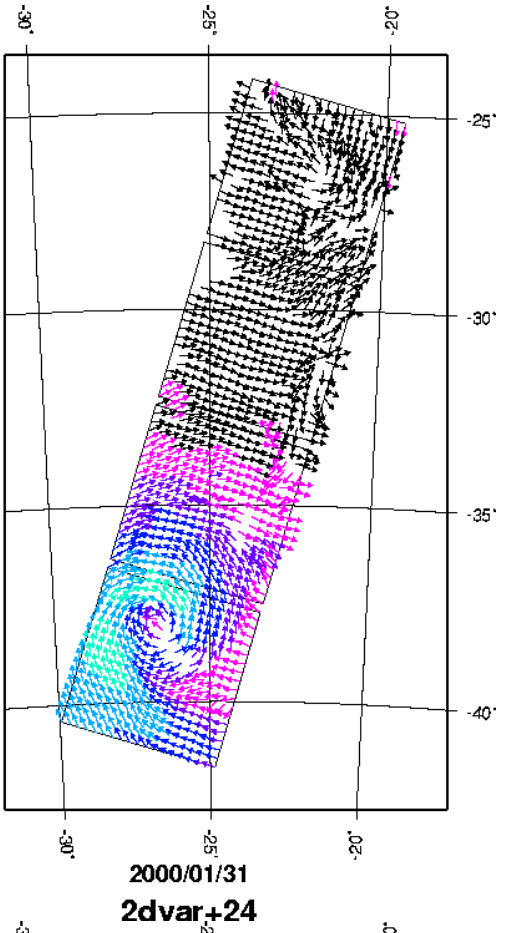
-30°
-25°
-20°
-25°
-30°
-35°
-40°
30
25
20
15
10
5
2000/01/31
2dvar+24

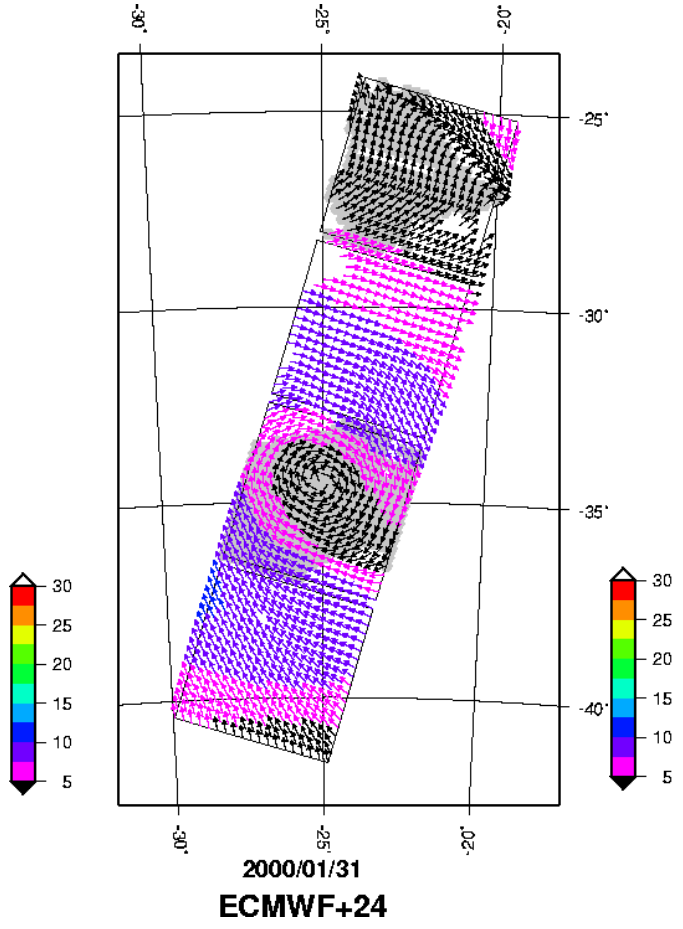
-30°
-25°
-20°
-25°
-30°
-35°
-40°
30
25
20
15
10
5
2000/01/31
ECMWF+24

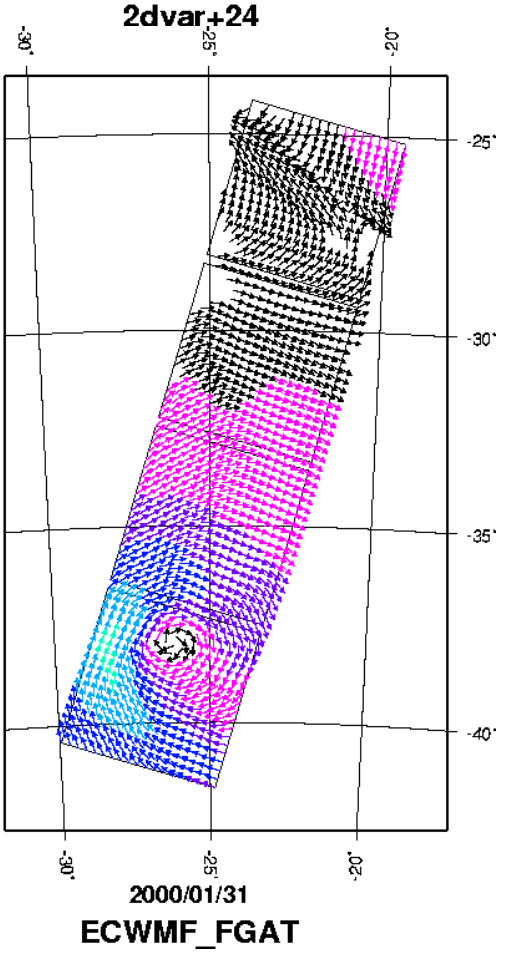
-30°
-25°
-20°
-25°
-30°
-35°
-40°
30
25
20
15
10
5
2000/01/31
ECWMF_FGAT